Development of an Advanced System for Automated 200 mm Wafer Mapping of Stress Using Test Structures

Development of an Advanced System for Automated 200 mm Wafer Mapping of Stress Using Test Structures

S. Lokhandwala, J. Murray, S. Smith, A.R. Mount†, J.G. Terry, A.J. Walton

Scottish Microelectronics Centre, Institute for Integrated Micro and Nano Systems, School of Engineering, The University of Edinburgh, Edinburgh, EH9 3FF, UK

†School of Chemistry, Joseph Black Building, The University of Edinburgh, EH9 3JJ, UK

***Abstract*— Controlling and understanding the stress in materials is of major importance in the successful fabrication of MEMS devices. Failure to properly account for stress related effects can lead to the substrate warping and layer delamination, both of which are detrimental to the performance and reliability of components. Hence, it is desirable to have reliable and automated technology to spatially monitor both stress and strain on silicon wafers. This paper reports in detail an integrated measurement system that has been specifically designed to semi-automatically wafer map stress, strain and Young's modulus. The measurement system is designed to determine the rotation of a test structure automatically and then calculate the strain. Young's modulus is then determined using a nanoindenter running customised software and the combination of the two measurements from the same location is used to calculate and map the spatial stress in the film.**

I. INTRODUCTION

Stress in deposited films is an important parameter that can have a critical effect on the performance and reliability of MEMS devices. This is especially the case when thick layers of materials are required and it is important to monitor and hence control stress to prevent cracking and delamination. Conventionally, wafer bow measurements [1,2] are used to monitor stress during fabrication. However, this has the limitation that, in many systems, an unpatterned wafer must be used and only a single measurement of stress is extracted. Unfortunately, this type of measurement provides no information on any spatial variation.

There have been many test structures reported for the characterisation of stress. For in-plane stress these can be divided into buckling and micro-rotating structures [3-10]. However, unlike most test structures designed for microfabrication process control, these structures are characterised optically rather than electrically and there are no commercially available systems to perform this task. As a result earlier versions of the in-house system reported in this paper have been used for measuring the angle of micro-rotating test structures. These results have been presented in a number of papers [7,8,11,12], with one of them describing manual measurements of Young's modulus using a nanoindenter (65 measurements), which were then combined with strain measurements to wafermap stress [13]. This paper focuses on reporting the development of;

(i) a measurement system to automatically measure the test structure's rotation and

(ii) the modifications to a commercial nanoindenter system required to wafer map Young's modulus,

neither of which have been previously reported in any detail. The automation and integration of the two measurements provides a new and more robust capability to rapidly wafer map stress. Amongst other things the paper describes the methods used to minimise the need for the user to tune and calibrate the system before use, as well as automatically identifying and categorising structures that are non-functional so that these results can be tagged and discounted, as appropriate, without the need for manual intervention. The paper also gives information on the repeatability of measurements and their sensitivity to system parameter setting.

II. STRESS MEASUREMENT TEST STRUCTURES

As it has been mentioned previously many papers have been published on stress/strain test structures [3-13]. With their angle of rotation being characterised optically the measurement of these micro-rotating structures is normally a largely manual process, which involves visually determining the angle of a pointer arm. This procedure is both time consuming and prone to error and, if the spatial variation of stress over a wafer is desired, then routinely characterising hundreds of stress sensors on a wafer is impractical. Hence, there is a requirement for automated systems which can rapidly and reliably extract the angle of rotation of large numbers of strain structures.

Fig. 1 shows a schematic of the test structure for which the measurement system has been designed. The offset expansion arms in this case result in clockwise rotation for tensile stress and anti-clockwise for compressive stress [8]. The design of the hinges where the expansion arms attach to the pointer arms is an important parameter that affects the angle of rotation [8].

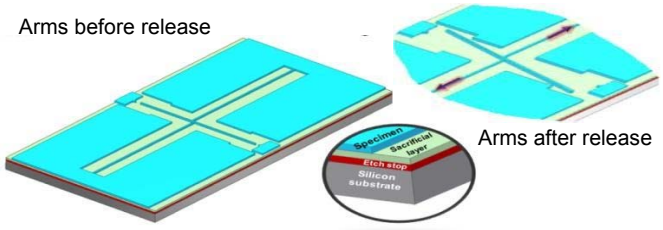

Fig. 1. Strain test structure. Under stress the arms relax by rotating uniaxially. Clockwise rotation indicates **tensile** stress, while anticlockwise rotation indicates **compressive** stress

978-1-4673-XXXX-X/17 $XX.XX © 2017 IEEE

Knowledge of the angle the pointer arm rotates can be used to extract the layer strain and reference [12] details how this can be achieved by using simulation in conjunction with experimental measurement.

III. THE STRESS MEASUREMENT SYSTEM

The integrated measurement system reported in this paper is comprised of two elements that have the following functions

1. **Measurement of the test structure rotation** (a wafer mapping camera attached to a microscope on a semi-automatic prober integrated through LabVIEW). This system takes a photograph of each structure using the prober to step to every test structure site on the wafer
2. **Measurement of Young's modulus** (nanoindenter with a 200 mm wafer chuck). This system steps a nanoindenting diamond tip to the same locations as all the strain structures that have been imaged.

The following sections describe the elements of the measurement system in more detail.

A. Measurement of test structure rotation

The measurement setup shown in Fig 2 is integrated through LabVIEW and has been designed to be semi-automated with a GUI (Graphical User Interface) based wafer mapping capability forming an integral part of the system. This enables the mapping of individual structures across a complete wafer. The software also provides a click and drag option, which allows the user to initially set the system up to select the test chips and test structures to be characterised. After creating the measurement coordinates, the software translates the test structure coordinates on each chip into a prober compatible coordinate array. This information is also directly used for the nanoindenter wafer mapping so that Young's modulus measurements can be made in close proximity to the strain test structures.

As the system is automated it needs to perform initialisation checks before commencing any photographic capture of test structure images. Having been designed for acquiring accurate images at high speed, the system monitors the following parameters both initially and during the measurements process to optimise the performance of the image processing and pattern recognition. These are the prober GPIB‡ read/write, chuck related settings (vacuum, offsets, x y z-axis crash control) and the camera settings (firewire port, image buffers, autofocus thresholds, image brightness, contrast and gamma adjustments).

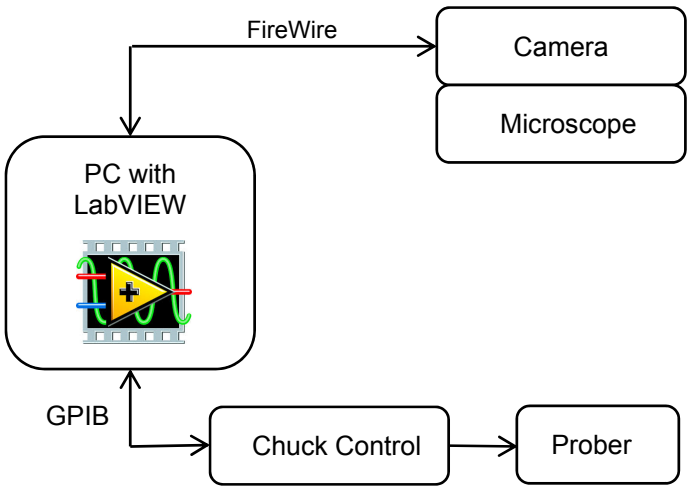

Fig 2. Block diagram of strain measurement system to measure rotation of the test structure

One of the major challenges has been the development of image processing software that enables many of the above parameters to be automatically set by the system without the requirement for user interaction. The initial version of the system software required significant user expertise to determine the best lighting conditions to optimise the edge detection algorithm's ability to identify the required edges of the pointer arm.

In the current implementation the camera is mechanically focused by the z-motion of the wafer chuck and uses software analysis of the image to determine the optimum focus. A focused image is very important for ensuring robust image processing analysis which can reliably extract the angle of rotation. Ideally, the camera should be focused at each site just before image capture, to eliminate the effect of wafer related parameters such as bow and the planarity of the chuck movement. Currently, the wafer chuck focusing procedure takes few minutes compared with the rest of the measurement time of few seconds (chuck x-y movement, settle time and image capture).

The software gives the option of focusing at every site or every *n*th image. For the 200 mm wafer design [7] this results in a scan time of 15 hours for a total of 12,288 structures (32 structures per chip) with focusing on 384 structures (one structure per chip). Clearly wafer mapping could be performed much more rapidly with an auto focus camera on the prober, which is an essential feature if speed of measurement is an important parameter.

Once all the images have been captured and stored in a folder the images can be analysed off-line. Fig 3 shows the image processing flow diagram. The first step in the process to convert the image into a black and white format making the detection of edges more effective by improving contrast levels and the separation of objects from the background. An example of the image resulting from this process is shown in Fig. 4.

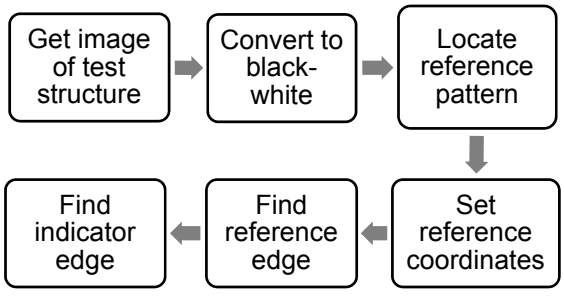

Fig 3. Image processing algorithm

‡ GPIB: General Purpose Interface Bus, IEEE-488 interface standard.

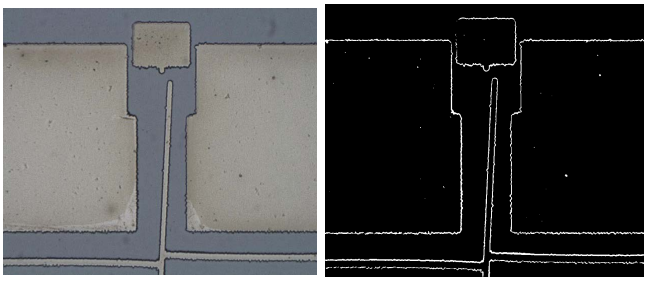

Fig 4. Image captured (left) and converted to black and white to identify the edges (right)

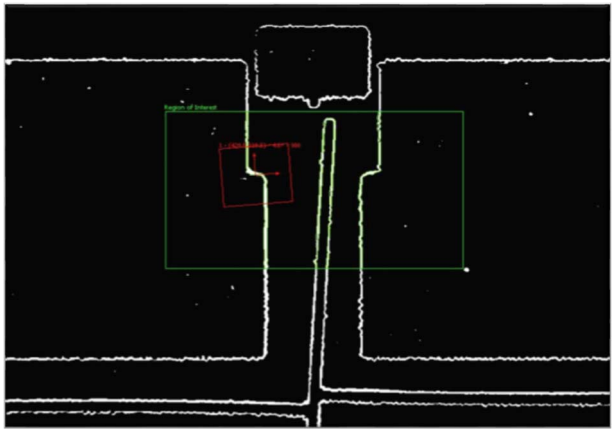

Fig. 5. Edges extracted from the photographic image by the system software

The next step is to identify the reference pattern, which is set by the user. Fig 5 gives an example a reference pattern identified by the system (red box) together with the region of interest (green box) for the pattern detection software to process. This image is the one on which the edge detection algorithm is applied to extract the angle of rotation.

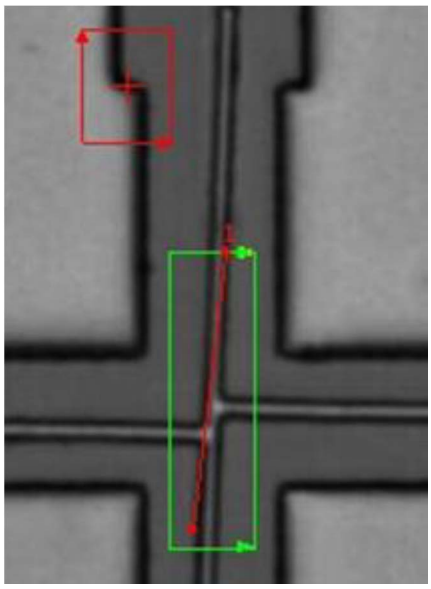

Fig. 6. Example of the edge detection algorithm failing to identify the right hand edge of the pointer arm

However, sometimes because of the quality of the picture (exposure, lighting, focus etc) the image processing algorithm resulted in the incorrect detection of reference patterns or edges. This in turn leads to incorrect measurements of the rotation angle. For example it can be observed from Fig. 6 that the detection of pointer arm does not pick-up a single edge and this results in the incorrect angle being extracted. Fortunately such errors can be simply identified by plotting the distribution of the angles extracted as shown in Fig 7†. The bimodal distribution is a characteristic of this problem and it is a simple matter to remove this invalid data from the analysis. Hence, the software facilitates this by enabling the user to set the range of the data to be removed. The disadvantage of this approach is that measurements of many correctly functioning structures are not available and clearly a better solution is to improve the edge detection image processing algorithm to make it less sensitive to parameters set by the software and the user.

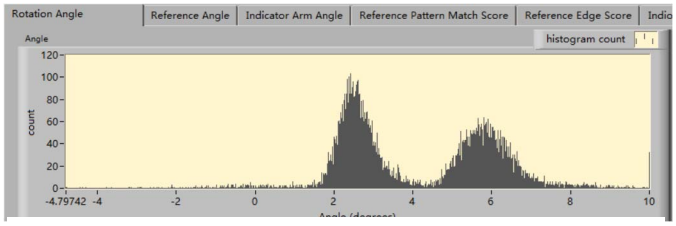

Fig. 7. The bimodal distribution it the extracted angle of rotation resulting from incorrect edge detection as shown in in Fig. 6 [14].

This issue was resolved by the use of an auto-threshold algorithm, which much improved the system's immunity to the changes in lighting level of the image. To further improve the detection of the reference pattern a geometric matching algorithm was also implemented so that effects such as pixel intensity, occlusion, shift and rotation in the image had no detrimental effect on the analysis. These improvements significantly increased the measurement fidelity of functioning strain indicators which is quantified later. It also facilitated the ability of the system to correctly categorise faulty structures and remove them from any data analysis.

The system can highlight the location of faulty structures by indicating their existence on wafer maps. When these structures are selected with the cursor the user is presented with the photographic image, and provides the option to over-ride the automated system categorization, if appropriate.

Fig 8 shows a histogram of the rotation angle measurements of 12,288 structures on a 200 mm Ni plated wafer. Note the zero angle measurements are non-functional structures, which are

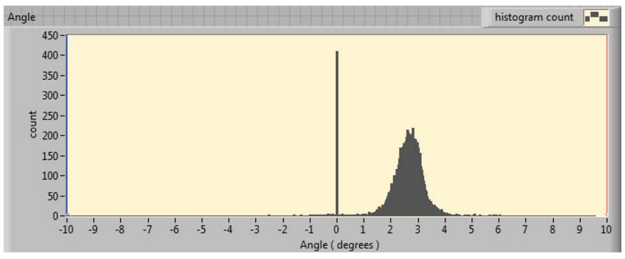

Fig. 8. Histogram of extracted rotation angles for 12,288 structures on a 200 mm Ni plated wafer.

† Other parameter distributions which can be plotted include reference angle, indicator arm angle, reference pattern match score, reference edge score and indicator edge score.

automatically removed from the data analysed (this can also be manually over-ridden).

B. Young's Modulus measurement

The nanoindenter used as part of the stress measurement system is a Keysight G200 system, which can be programmed to measure Young's modulus in the anchor area of the structures shown in Fig 1. The system is equipped with a custom 200 mm chuck that can rotate through ±180º, which enables a 200 mm wafer to be mapped in Cartesian coordinates (in a similar manner to that used during the optical test structure measurements) by rotating the wafer appropriately (this is facilitated by the nanoindenter probe not being located in the centre of the scan area). At the present time the measurement capability has been implemented in four scanning blocks as shown in Fig 9, which measures all but 16 chips on the wafer. Full 200 mm semi-automated wafer scanning simply requires extra small scanning blocks to be added to the software. Fig 10 shows a preliminary example wafermap (one structure per chip) of Young's modulus measurements for a Permalloy film electroplated on a 200 mm wafer.

C. System performance

As mentioned previously the latest version of the software has automated algorithms to detect non-functional structures (e.g. missing and broken structures such as one shown in Fig 11) as well as images that cannot be processed, and categorises them. Table 1 gives some of the categories and their status codes that are identified by the software. Fig 12 shows a wafer map of these status codes for the user to navigate and verify pictures of the non-functional structures using the cursor, should they so wish. Figure 13 shows a wafermap of strain measurement themselves with the black regions indicating status codes greater than 0 or areas with no strain structures.

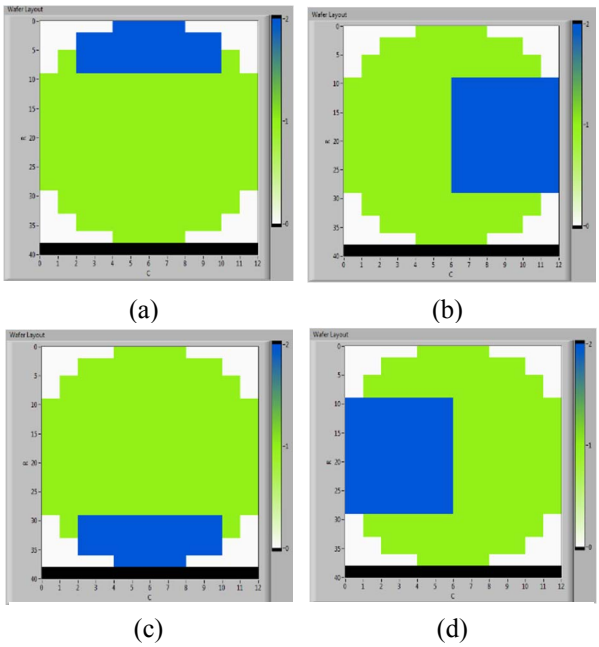

Fig 9. Regions selected for measurements on a 200 mm wafer, (a) 0°, (b) 90°, (c) 180° and (d) 270°.

Table 2 summarises this data and indicates that 95.93% of structures have the expected pattern and are candidates to be measured. The 2.28% structures with the status code of 'indicator edge not detected' are structures with broken indicator arms. This can be due to damage caused by handling during and/or after fabrication or mask related defects. The structure status wafer map shown in Fig 12 has two vertical purple bands, both of which are known to be related to mask defects.

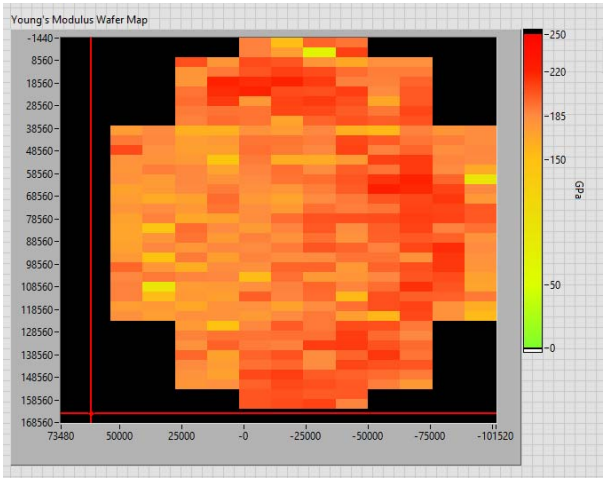

Fig 10. Wafer map of Young's modulus for a 200 mm wafer. Note: questionable data has been replaced with averaged with neighbouring data

TABLE 1. STRUCTURE CATEGORIES AND THEIR ASSOCIATED CODES

Status code	Category
0	No error i.e. angle extracted correctly
1	Reference pattern was not found
2	Reference edge was not detected
3	Indicator edge was not detected
4	Reference edge score not in user defined range
5	Indicator edge score not in user defined range

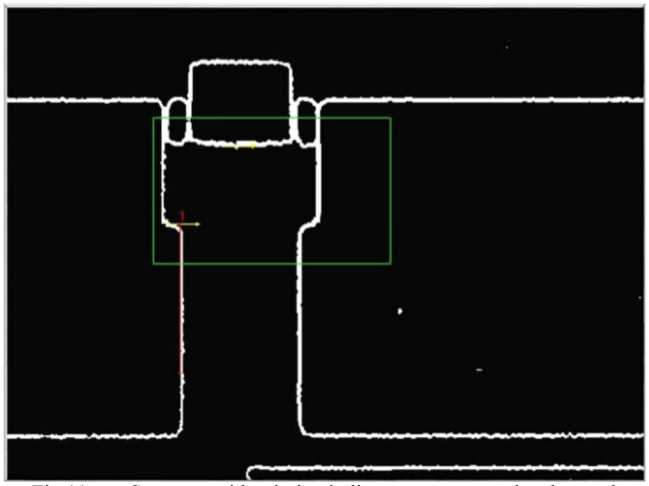

Fig 11. Structure with missing indicator arm so no edge detected (status code 3).

TABLE 2. PERCENTAGE OF STRUCTURES TOGETHER WITH THEIR STATUS CODES EXTRACTED BY THE SOFTWARE.

Status code	No. of structures	% of structure
0	11788	95.93
1	79	0.64
2	19	0.15
3	280	2.28
4	118	0.96
5	4	0.04

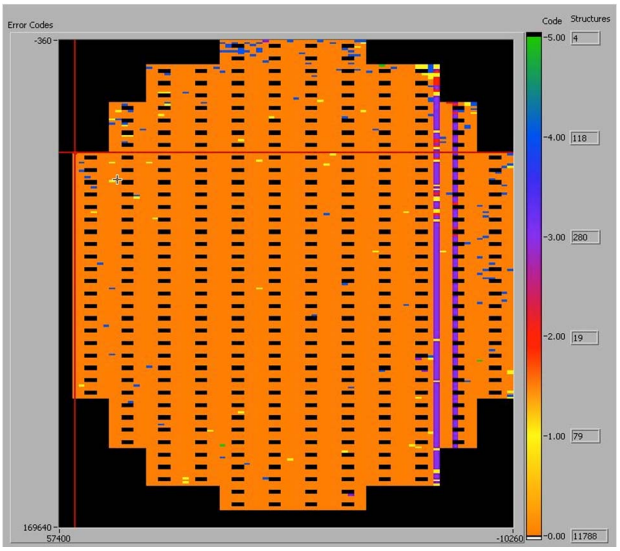

Fig 12. Wafer map of status codes of test structures.

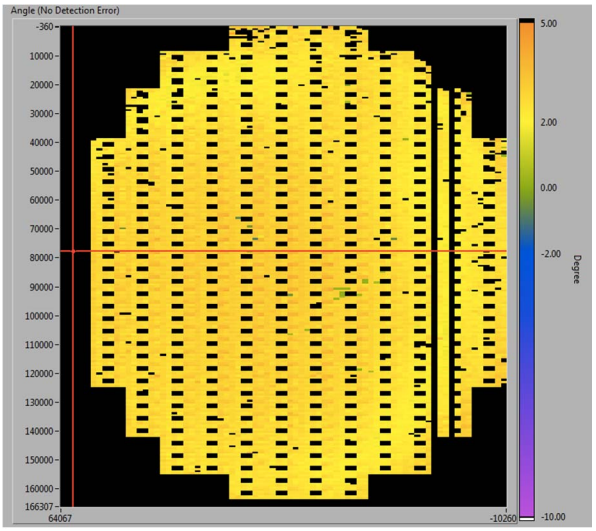

Fig 13. Angle of rotation/strain measurements wafer map (12,288 structures)

Clearly, the system should perform its measurement task identically each time the same wafer is photographed. To evaluate the robustness of this process the same wafer was measured 9 times, which included loading onto the chuck, theta alignment and varying the light adjustment over a wide range. This procedure resulted in 96.4% of all the 12,288 structures being allocated the same status codes. Compared with the

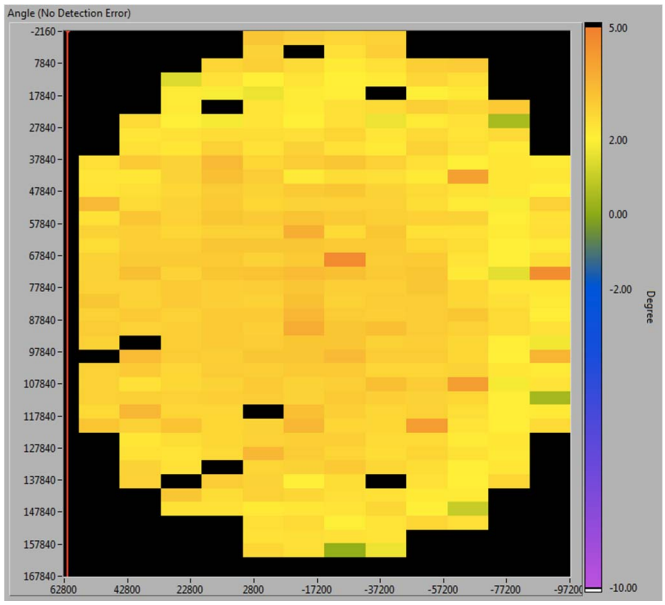

Fig 14. Angle of rotation/strain measurements (384 structures) corresponding to the position of the Young's modulus measurements (Fig 10).

image processing results presented discussed previously this is a major improvement over the earlier versions of the software, which required the manual identification of all "outlier" data on the wafer map. This procedure involved the user tagging the structure/measurement as faulty for a displayed image of the selected test structure (this manual system is still available to augment the automated process, and provides the ability to check the performance of the automated procedure).

Using the same images as those recorded above for categorising structures an evaluation was performed comparing the angles of rotation extracted to provide information about the repeatability of these measurements. Table 3 summarises this data with 97.7% of the repeated measurement on the same structure being within ±0.2°. These results provide confidence that the system is able to correctly identify functioning structures and measure over 97% of these with a repeatability of ±0.2°

IV. WAFER MAPPING OF STRESS DATA

Fig 14 shows a strain measurement wafermap at the same positions as the Young's modulus measurements with Fig 15 presenting a wafer map of stress data extracted by combining the strain (Fig 14) and Young's modulus data (Fig 10). This demonstrates the power of the measurement system, which transforms MEMS based, stress characterisation devices from being interesting structures with limited quantitative information

TABLE 3. REPEATABILITY OF MEASUREMENTS FOR 9 DIFFERENT WAFER SCANS

Tolerance range (°)	No of structures in tolerance range	% structures in tolerance range
0.1	9,912	83.6%
0.2	11,584	97.7%
0.3	11,765	99.3%
0.4	11,814	99.7%
0.5	11,822	99.8%
1.0	11,833	99.8%

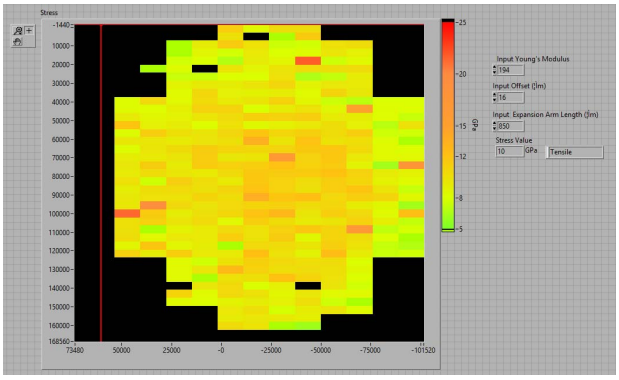

Fig 15. Wafer map of residual stress computed using Young's modulus (Fig 10) and the measured angle of rotation (Fig 14).

onto another level. This approach not only provides quantitative information but also increases the volume of data that can be routinely extracted. This opens up the possibility of routinely creating wafer maps, which has not been previously feasible. An additional appeal of the system is that the nanoindenter only requires very small areas of the anchor regions to extract Young's modulus and the strain measurement component is completely non-contact, and so again no area is required for probe pads.

V. CONCLUSIONS

This paper has described the implementation of an automated high speed measurement system capable of extracting results from over 12,000 micro rotating test sensors structures. This makes it feasible to comprehensively map the stress over many wafers when developing new processes, which is a significant advance over a manual extraction of the rotation angle, which is both error-prone and laborious.

It clearly demonstrates that the strain structures *together* with the ability to automatically and reliably measure the angle of rotation is able to reveal spatial stress variation when combined with Young's modulus from the modified nanoindenter. Without this combination and the customised 200 mm wafer chuck on the nanoindenter the wafer mapping of stress demonstrated in this paper is simply not a realistic proposition.

The capability of the resulting system has been demonstrated by measuring the pointer arm rotations in structures fabricated from ~5µm thick electroplated Ni. However, it should be noted that the system is not material specific and has been successfully used for NiFe, Cu, Parylene, and SU-8 films.

Wafer maps have been shown which demonstrate the potential of the system to extract spatial variation. It provides the capability to perform more comprehensive experiments to characterise the spatial variation of stress in different materials. This will consequently help optimise the performance of these micro-rotating test structures and help provide a deeper understanding of the origin and distribution of stress within materials.

ACKNOWLEDGEMENTS

The authors would like to acknowledge the support of EPSRC/IeMRC, a Spirit Studentship, and EPSRC (FS/01/02/10) IeMRC Flagship Project on Smart Microsystems. The authors would also like to acknowledge contributions by D. Pak, F. Deng and Y. Jia who have contributed towards elements of the software related to the measurement of strain. The data reported in this paper is available from DOI: http://hdl.handle.net/10283/2342

REFERENCES

[1] G.G. Stoney, "The Tension of Metallic Films Deposited by Electrolysis", Proc. R. Soc. Lond. A, vol 82, pp 172-175, 1909

[2] G.C.A.M. Janssen, M.M. Abdalla, F. van Keulen, B.R. Pujada, B. van Venrooy, "Celebrating the 100th anniversary of the Stoney equation for film stress:Developments from polycrystalline steel strips to single crystal silicon wafers", Thin Solid Films, vol 517, pp1858–1867, 2009

[3] H. Guckel, D. Burnst, C. Rutigliano, S.E. Lovell, B. Choi, "Diagnostic microstructures for the measurement of intrinsic strain in thin films", J. Micromech. Microeng., Vol 2, pp 86-95, 1992

[4] H. Guckel, T. Randazzo, D.W. Burns D W, "A simple technique for the determination of mechanical strain in thin films with application to polysilicon", J. Appl. Phys., vol 57, 1671–5, 1985

[5] Y.B. Gianchandani, K. Najafi, "Bent-Beam Strain Sensors", Journal of Microelectromechanical Systems, Vol. 5, No. 1, pp52-58, March1996

[6] M.G. Allen, M. Mehregany, R.T. Howe, S.O. Senturia, "Microfabricated structures for the in-situ measurement of residual stress, Young's modulus, and ultimate strain of thin films", Appl. Phys. Lett., 51, pp. 241-243, 1987.

[7] S. Smith, N.L. Brockie, J.G. Terry, N. Wang, A. Horsfall, A.J. Walton, "Application of a Micromechanical Test Structure to the Measurement of Stress in an Electroplated Permalloy Film", IEEE International Conference on Microelectronics Test Structures, Edinburgh, pp. 75-80, March 2009.

[8] J.G Terry, S. Smith, A.J Walton, A.M Gundlach, J.T.M Stevenson, A.B Horsfall, K. Wang, J.M.M dos Santos, S.M Soare, N.G Wright, A.G O Neill, S.J. Bull; "Test Chip for the Development and Evaluation of Test Structures for Measuring Stress in Metal Interconnect", IEEE Trans. Semiconductor Manufacturing, pp. 255-261, May 2005

[9] X. Zhang, T-Y. Zhang, Y. Zohar; "Measurements of residual stresses in thin films using micro-rotating-structures", Thin Solid Films, vol. 335, pp. 97-105, 1996.

[10] B.P van Drieehuizen, J.F.L Goosen, P.J. French, R.F. Wolffenbuttel, "Comparison of Techniques for Measuring Both Compressive and Tensile Stress in Thin Films", Sensors Actuators, A37-38, p756, 1993.

[11] S. Smith, N.L. Brockie, J. Murray, C.J. Wilson, A.B. Horsfall, J.G. Terry, J.T.M. Stevenson, A.R. Mount, A.J. Walton, "Fabrication of Test Structures to Monitor Stress in SU-8 Films used for MEMS Application, IEEE International Conference on Microelectronics Test Structures, Hiroshima, pp 8-13, March 2010

[12] S. Smith, N.L. Brockie, J. Murray, C.J. Wilson, A.B. Horsfall, J.G. Terry, J.T.M. Stevenson, A. R. Mount, A.J. Walton, "Analysis of the Performance of a Micromechanical Test Structure to Measure Stress in Thick Electroplated Metal Films", IEEE International Conference on Microelectronics Test Structures, Hiroshima, pp 80-85, March 2010

[13] G Schiavone, J Murray, S Smith, M P Y Desmulliez, A R Mount, A J Walton, "A wafer mapping technique for residual stress in surface micromachined films", J. Micromech. Microeng. 26(2016) 095013, doi:10.1088/0960-1317/26/9/095

[14] F. Deng, "Enhanced measurement of stress test structures", MEng thesis, University of Edinburgh, 2015